Supplementary Information (SI) for Nanoscale.

Electronic Supplementary Information

Pyrazinium Ionic Liquid for Preparing A 0D/2D Hybridized N, P-codoped Carbon Enriched with Pyridinic N and Enhanced Electrocatalytic Performance toward Oxygen Reduction Reaction

Jian Gao[a,b], Yuejiao Sun[a], Na Ma[c], Yunyuan Chu[a], Hong Wang[a], Hanmin Tian[d*], Zhen Yin[b,c*], Xiaoyao Tan[a], and Peng Zhang[b,e*]

[a] State Key Laboratory of Separation Membranes and Membrane Processes, School of Chemical Engineering and Technology, Tiangong University, Tianjin 300387, China

[b] Haian Nanjing University High Tech Institute, Haian 226600, China

[c] College of Chemical Engineering and Materials Science, Tianjin University of Science and Technology, Tianjin 300457, China

[d] School of Electronics and Information Engineering, Hebei University of Technology, Tianjin 300400, China.

[e] School of Environmental Science and Engineering, Tiangong University, Tianjin 300387, China

*Corresponding Author.

E-mail: tianhanmin@hebut.edu.cn (Hanmin Tian).

E-mail: yinzhen@tust.edu.cn (Zhen Yin).

E-mail: pengzhang@tiangong.edu.cn (Peng Zhang).

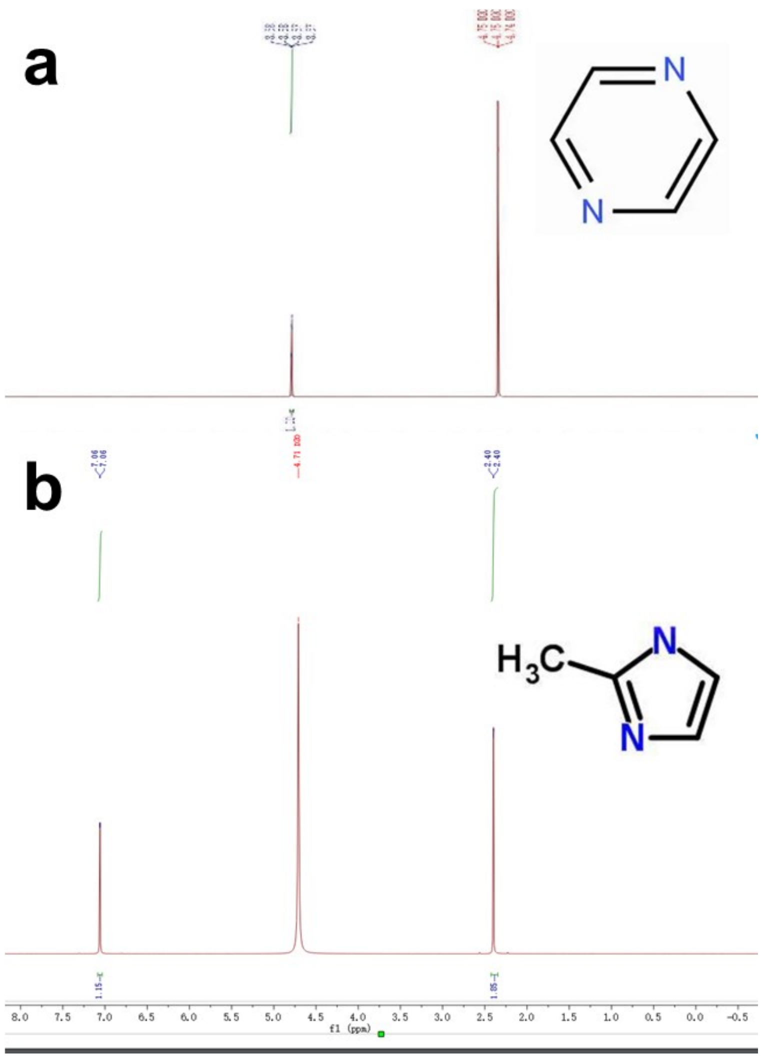

Fig.S1 ^{1}H NMR for (a) [Hpyraz]H_2PO_4 and (b) [2-Mim]DHP.

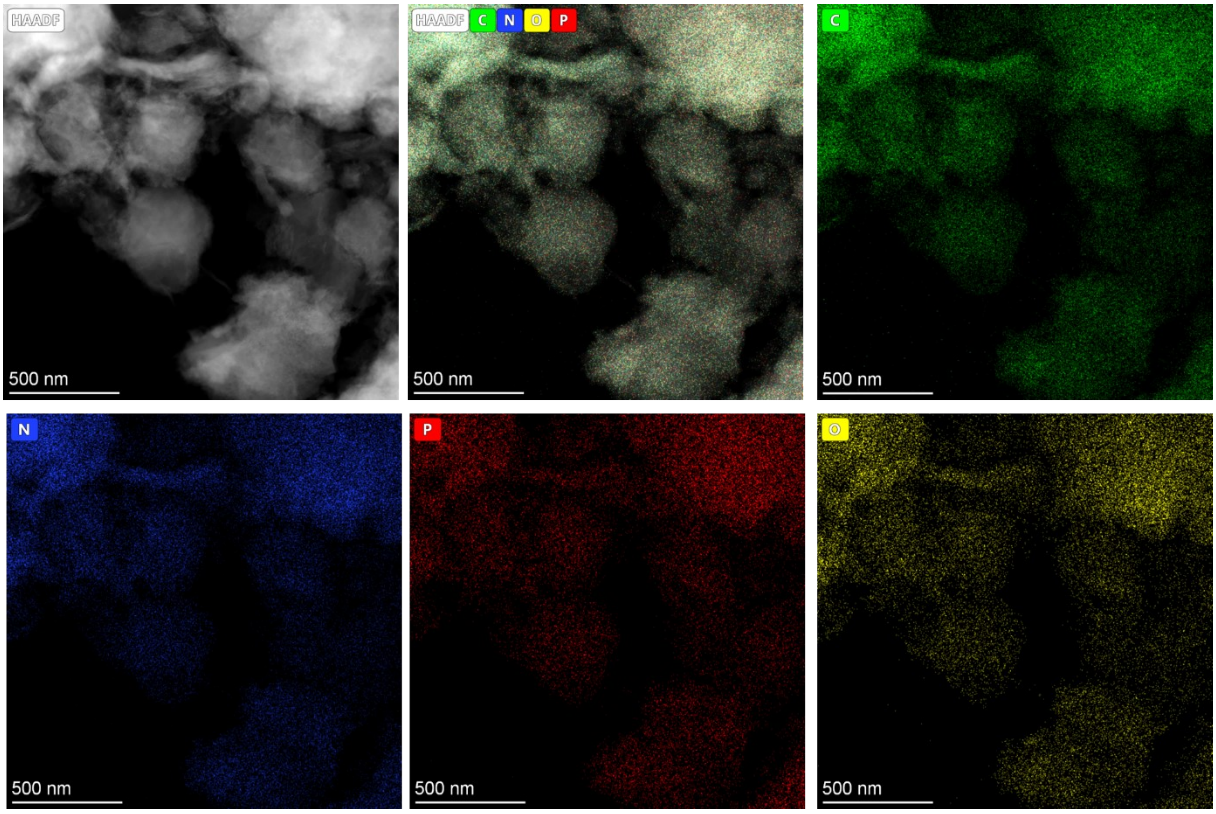

Fig. S2 HAADF STEM image of C_{mim} and corresponding EDS elemental mappings.

Table S1 Weight contents of C, N, and H in the C_{pyr} and C_{mim} obtained by EA results

Sample	C (wt. %)	H (wt. %)	N (wt. %)
C_{mim}-700	76.74	1.16	1.89
C_{mim}-800	85.38	0.59	0.95
C_{mim}-900	89.43	0.36	0.24
C_{mim}-1000	89.23	0.29	0.24
C_{pyr}-700	85.07	0.52	0.16
C_{pyr}-800	91.23	0.30	0.19
C_{pyr}-900	90.34	0.40	0.17
C_{pyr}-1000	89.13	0.31	0.10

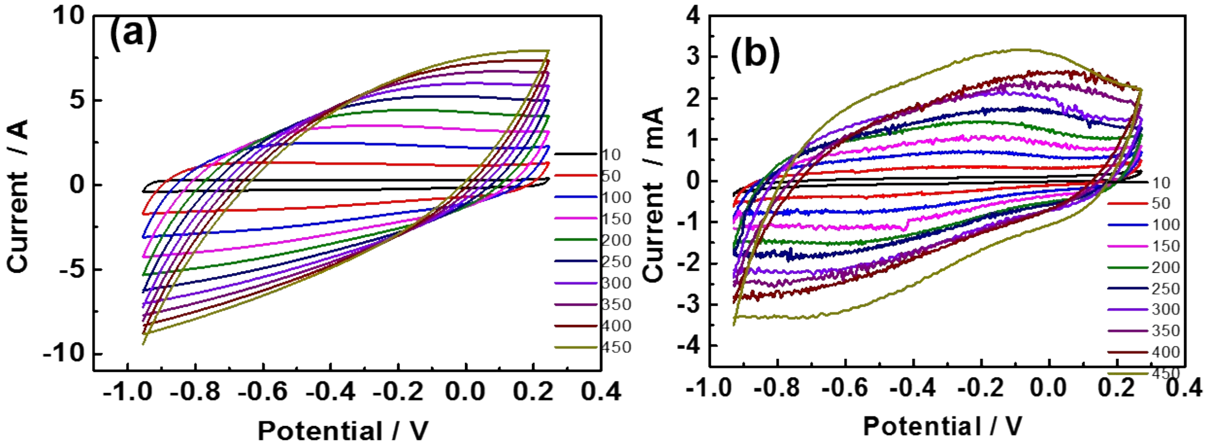

Fig. S3 CV curves for (a) C_{pyr} and (b) C_{mim}.

Table S2 ORR performance of various catalysts reported in recent years.

	Catalyst	Precursor/condition	Onset Potential/ V_{RHE}	Half wave potential V_{RHE}	Specific current V_{RHE}	Reference
1	N-doped carbon	Silica-supported polyaniline/900 ºC, Ar, 2h	~0.94	0.71	4.8	1
2	N-Ketjenblack/Fe/Fe_3C-Functionalized Melamine Foam	$FeCl_2$, ketjenblack, melamine foam/800ºC, Ar, 2h	~0.93	0.78	12	2
3	N-doped carbon	Melamine/phenol formaldehyde (M-PF) resin/ 900 ºC, Ar, 3h.	~0.97	0.84	19.02	3
4	N-doped carbon	Ethyl linked bis(N-(2-cyanoethyl)-imidazole bis(pentafluoroethylsulfonyl)-imide/950 ºC, Ar, 2h	~0.95	0.80	18	4
5	N,P co-doped carbon	Polyaniline aerogel and phytic acid/1000 ºC, Ar, 2h	0.94	0.85	20.9	5
6	Fe-N-C-HNS-750	Fe^{3+}-PDA/SiO_2/750ºC, Ar, 2h	0.89	0.72	0.58	6
7	Graphene Quantum Dots/ Graphene Nanoribbons	Na, Methylbenzene, hexabromobenzene/1000ºC, Ar, 2h	~0.97	0.78	19.6	7
8	N-doped porous graphene foam	GO, $FeCl_2$, dicyandiamide, silica sphere/900 ºC, N_2 1h	1.02	0.86	12.4	8

9	N,P co-doped carbon	Melamine, phytic acid, graphene oxide/1000°C, Ar, 1h.	~0.95	~0.81	22.9	9
10	Graphene quantum dots	graphitized carbon nanofibers/120 °C, reflux, 2h	~0.84	0.67	1.3	10
11	Co_3O_4	$Co(NO_3)_2$, glycerol/700 °C, Ar, 200 min	0.93	0.84	13.7	11
12	N-doped carbon	polyimide (PI) film/1000 °C, Ar, 1h	0.97	0.82	29.4	12
13	N,S co-doped carbon	pyrrole, aniline, ammonium persulfate/various temperatures, N_2, 2	0.93	0.81	7.13	13
14	N-doped carbon	ZIF-67, 900 °C, N_2, 1h.	0.91	0.84	37.8	14
15	Co-N-doped Hollow Carbon Spheres	poly(methyl methacrylate), cobalt acetate/800 °C, N_2, 5h	0.96	0.86	16.7	15
16	N-doped GO	GO/5 °C, ultrasonic treatment, 5 min	0.84	0.7	0.98	16
17	Co-N-C	$Co(NO_3)_2$, $HvimNO_3$/600 °C, N_2, 1h	0.96	0.8	7.85	17
18	Mn_3O_4/Ti_3C_2	Ti_3C_2 Mxene, $Mn(AC)_2$ /150 °C, 3h	0.89	0.8	25	18
19	N,P co-doped carbon	$[Hvim]H_2PO_4$/560°C, N_2, 1h	0.93	0.75	7.7	19
20	Fe-N-C	$(Fe(NO_3)_3$, nicarbazin, methylimidazole, glucoril , zinc, carbon nanotube and LM150 fumed silica/975 °C, N_2, 45 min	0.96	0.83	10.7	20
21	N, P dual-doped carbon	melamine–diphenylphosphinic acid/1100 °C, N_2, 1h	0.91	0.79	7.85	21
22	N, S copded carbon	Acetylene black, melamine and sluphur template/900 °C, vacuum, 1h	0.99	0.82	9.44	22
23	N-doped holey carbon	GO, zinc gluconate/900 °C, Ar	0.97	0.82	17.6	23
24	Fe-N-C	glycine, citric acid, and $FeCl_3$ /800 °C, N_2, 2h	0.93	0.75	8	24
25	Graphdiyne doped with N	few-layer oxidised graphdiyne, melamine/900 °C, Ar, 3h	~1.0	0.87	9.32	25
26	Pyridinic-N-doped graphene	C_3N_4-GO/900 °C, N_2, 3h	0.98	0.85	27.2	26
27	FeN_4 Moiety/ MXene	Ti_3C_2Tx MXene and FePc/ stirred 20h	~0.93	0.86	20.8	27
28	Fe-N_4-carbon fabric	GO, polyacrylonitril, $FeCl_3$/900 °C, NH_3, 1h	0.93	0.73	Not Available	28
29	N-doped carbon	Citric acid and NH_4Cl/1000 °C,	0.95	0.82	19.62	29

		Ar, 3h				
30	N-doped porous carbon	D-gluconic acid sodium/700°C, Ar, 1h	0.94	0.864	19	[30]
31	N-doped porous carbon	Bio-MOF-1 $Zn_8(Ad)_4(Bpdc)_6O{\cdot}2Me_2NH_2{\cdot}8DMF{\cdot}11H_2O$/1000°C, Ar, 1,2,3,4h.	0.96	0.84	9	[31]
32	S,N,F triple-doped carbon	Superfine PTFE, thiourea/800 °C,Ar,1h	0.98	0.86	11.77	[32]
33	Pichlorohydrin-dimethylamine copolyme modified CNT	Pichlorohydrin-dimethylamine copolyme modified CNT/700 °C, 24h	0.87	0.7	0.2	[33]
34	N-doped CNT in Fe-Nx/Fe_2O_3/Fe_3O_4-encapsulated carbon sheet	Fe-Nx/Fe_2O_3/Fe_3O_4-encapsulated carbon	0.95	0.85		[34]
35	N, P-doped carbon	[H2pyraz]2H_2PO_4/900 °C, N_2, 1h	0.93	0.75	3.0	This work

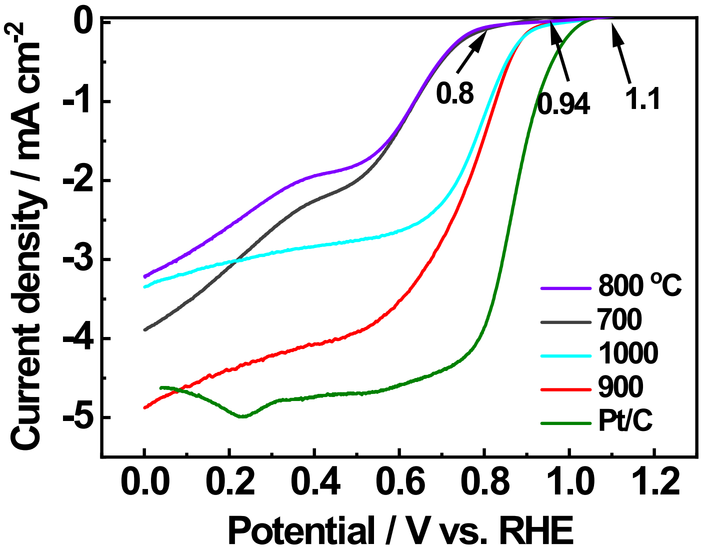

Fig. S4 LSVs for C_{pyr} prepared at various temperatures.

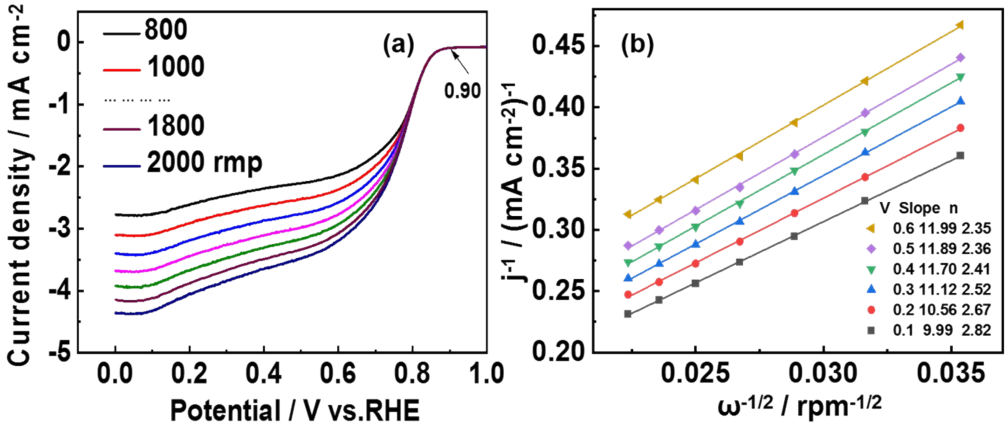

Fig. S5 (a) LSV curves at various rotational speeds for C_{mim}, (b) K-Lplots for C_{mim}.

Table S3 Peak power density of ZABs with some reported ORR catalyst

	Catalyst	PPD ($mW \cdot cm^{-2}$)	Reference
1	Pt/C+RuO_2	80	[34]
2	Fe, N-doped 3D porous carbon	112	[35]
3	Pt/MoC/ nitrogen-doped carbon	100	[36]
4	Pt/C+RuO_2	50	[37]
5	Conjugated aromatic/Co-Fe	88	[38]
6	N,P co-doped carbon	117	This work

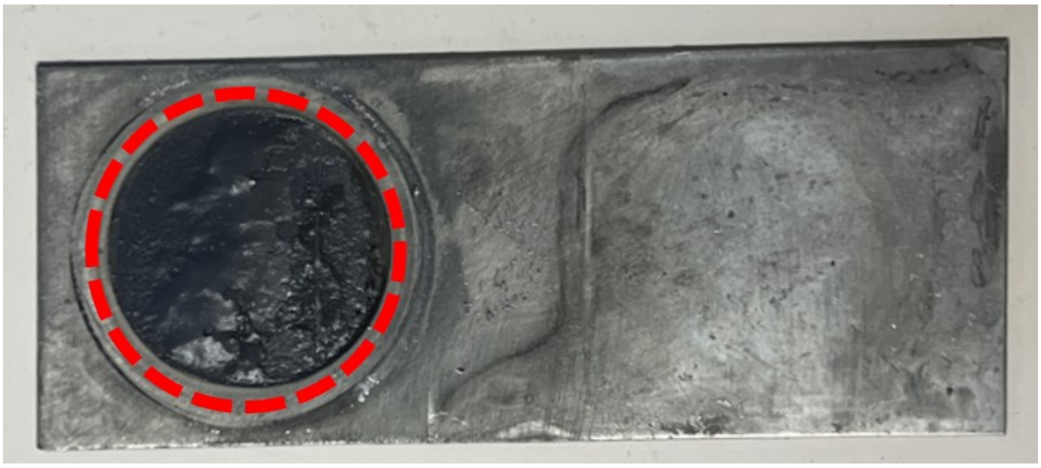

Fig. S6 Picture of the Zn foil after discharging for 4 hours, the circled area is the working area.

References

(1) Silva, R.; Voiry, D.; Chhowalla, M.; Asefa, T. Efficient metal-free electrocatalysts for oxygen reduction: polyaniline-derived N- and O-doped mesoporous carbons. *J. Am. Chem. Soc.* **2013,** *135*, 7823-7826.

(2) Lee, J. S.; Park, G. S.; Kim, S. T.; Liu, M. L.; Cho, J. A Highly Efficient Electrocatalyst for the Oxygen Reduction Reaction: N-Doped Ketjenblack Incorporated into Fe/Fe_3C-Functionalized Melamine Foam. *Angew. Chem. Int. Ed.* **2013,** *52*, 1026-1030.

(3) He, W.; Jiang, C.; Wang, J.; Lu, L. High-Rate Oxygen Electroreduction over Graphitic‐N Species Exposed on 3D Hierarchically Porous Nitrogen‐Doped Carbons. *Angew. Chem. Int. Ed.* **2014,** *53*, 9503-9507.

(4) Zhang, Z. Y.; Veith, G. M.; Brown, G. M.; Fulvio, P. F.; Hillesheim, P. C.; Dai, S.; Overbury, S. H. Ionic liquid derived carbons as highly efficient oxygen reduction catalysts:

first elucidation of pore size distribution dependent kinetics. *Chem. Commun.* **2014,** *50*, 1469-1471.

(5) Zhang, J.; Zhao, Z.; Xia, Z.; Dai, L. A metal-free bifunctional electrocatalyst for oxygen reduction and oxygen evolution reactions. *Nat. Nanotechnol.* **2015,** *10*, 444-452.

(6) Zhou, D.; Yang, L.; Yu, L.; Kong, J.; Yao, X.; Liu, W.; Xu, Z.; Lu, X. Fe/N/C hollow nanospheres by Fe(iii)-dopamine complexation-assisted one-pot doping as nonprecious-metal electrocatalysts for oxygen reduction. *Nanoscale* **2015,** *7*, 1501-1509.

(7) Jin, H. L.; Huang, H. H.; He, Y. H.; Feng, X.; Wang, S.; Dai, L. M.; Wang, J. C. Graphene quantum dots supported by graphene nanoribbons with ultrahigh electrocatalytic performance for oxygen reduction. *J. Am. Chem. Soc.* **2015,** *137*, 7588-7591.

(8) Zhou, X.; Bai, Z.; Wu, M.; Qiao, J.; Chen, Z. 3-Dimensional porous N-doped graphene foam as a non-precious catalyst for the oxygen reduction reaction. *J. Mater. Chem. A* **2015,** *3*, 3343-3350.

(9) Zhang, J.; Qu, L.; Shi, G.; Liu, J.; Chen, J.; Dai, L. N,P-Codoped Carbon Networks as Efficient Metal-free Bifunctional Catalysts for Oxygen Reduction and Hydrogen Evolution Reactions. *Angew. Chem. Int. Ed.* **2016,** *55*, 2230-2234.

(10) Wang, M. R.; Fang, Z.; Zhang, K.; Fang, J.; Qin, F. R.; Zhang, Z. A.; Li, J.; Liu, Y. X.; Lai, Y. Q. Synergistically enhanced activity of graphene quantum dots/graphene hydrogel composites: a novel all-carbon hybrid electrocatalyst for metal/air batteries. *Nanoscale* **2016,** *8*, 11398-11402.

(11) Li, G.; Wang, X. L.; Fu, J.; Li, J. D.; Park, M. G.; Zhang, Y. N.; Lui, G.; Chen, Z. W. Pomegranate-inspired design of highly active and durable bifunctional electrocatalysts for

rechargeable metal-air batteries. *Angew. Chem. Int. Ed.* **2016,** *55*, 4977-4982.

(12) Liu, Q.; Wang, Y.; Dai, L.; Yao, J. Scalable fabrication of nanoporous carbon fiber films as bifunctional catalytic electrodes for flexible Zn-Air batteries. *Adv. Mater.* **2016,** *28*, 3000-3006.

(13) Wu, Z.; Liu, R.; Wang, J.; Zhu, J.; Xiao, W.; Xuan, C.; Lei, W.; Wang, D. Nitrogen and sulfur co-doping of 3D hollow-structured carbon spheres as an efficient and stable metal free catalyst for the oxygen reduction reaction. *Nanoscale* **2016,** *8*, 19086-19092.

(14) Jia, G.; Zhang, W.; Fan, G.; Li, Z.; Fu, D.; Hao, W.; Yuan, C.; Zou, Z. Three‐Dimensional Hierarchical Architectures Derived from Surface‐Mounted Metal–Organic Framework Membranes for Enhanced Electrocatalysis. *Angew. Chem. Int. Ed.* **2017**.

(15) Cai, S.; Meng, Z.; Tang, H.; Wang, Y.; Tsiakaras, P. 3D Co-N-doped hollow carbon spheres as excellent bifunctional electrocatalysts for oxygen reduction reaction and oxygen evolution reaction. *Appl. Catal. B-Environ.* **2017,** *217*, 477-484.

(16) Tao, H.; Yan, C.; Robertson, A. W.; Gao, Y.; Ding, J.; Zhang, Y.; Ma, T.; Sun, Z. N-Doping of graphene oxide at low temperature for the oxygen reduction reaction. *Chem. Commun.* **2017,** *53*, 873-876.

(17) Gao, J.; Ma, N.; Zheng, Y.; Zhang, J.; Gui, J.; Guo, C.; An, H.; Tan, X.; Yin, Z.; Ma, D. Cobalt/nitrogen-doped porous carbon nanosheets derived from polymerizable ionic liquids as bifunctional electrocatalyst for oxygen evolution and oxygen reduction reaction. *ChemCatChem* **2017,** *9*, 1601-1609.

(18) Xue, Q.; Pei, Z.; Huang, Y.; Zhu, M.; Tang, Z.; Li, H.; Huang, Y.; Li, N.; Zhang, H.; Zhi, C. Mn_3O_4 nanoparticles on layer-structured Ti_3C_2 MXene towards the oxygen reduction

reaction and zinc-air batteries. *J. Mater. Chem. A* **2017,** *5*, 20818-20823.

(19) Gao, J.; He, C.; Liu, J.; Ren, P.; Lu, H.; Feng, J.; Zou, Z.; Yin, Z.; Wen, X.; Tan, X. Polymerizable ionic liquid as a precursor for N, P co-doped carbon toward the oxygen reduction reaction. *Catal. Sci. Tech.* **2018,** *8*, 1142-1150.

(20) Hossen, M. M.; Artyushkova, K.; Atanassov, P.; Serov, A. Synthesis and characterization of high performing Fe-NC catalyst for oxygen reduction reaction (ORR) in Alkaline Exchange Membrane Fuel Cells. *J. Power. Sources* **2018,** *375*, 214-221.

(21) Zhu, J.; Xiao, M.; Song, P.; Fu, J.; Jin, Z.; Ma, L.; Ge, J.; Liu, C.; Chen, Z.; Xing, W. Highly polarized carbon nano-architecture as robust metal-free catalyst for oxygen reduction in polymer electrolyte membrane fuel cells. *Nano energy* **2018,** *49*, 23-30.

(22) Xiang, Q.; Li, S.; Zou, X.; Qiang, Y.; Hu, B.; Cen, Y.; Xu, C.; Liu, L.; Zhou, Y.; Chen, C. Self-assembly porous metal-free electrocatalysts templated from sulfur for efficient oxygen reduction reaction. *Appl. Surf. Sci.* **2018,** *462*, 65-72.

(23) Sun, J.; Lowe, S. E.; Zhang, L.; Wang, Y.; Pang, K.; Wang, Y.; Zhong, Y.; Liu, P.; Zhao, K.; Tang, Z. Ultrathin Nitrogen‐Doped Holey Carbon@ Graphene Bifunctional Electrocatalyst for Oxygen Reduction and Evolution Reactions in Alkaline and Acidic Media. *Angew. Chem. Int. Ed.* **2018,** *130*, 16749-16753.

(24) Li, C.; He, C.; Sun, F.; Wang, M.; Wang, J.; Lin, Y. Incorporation of Fe3C and Pyridinic N Active Sites with a Moderate N/C Ratio in Fe–N Mesoporous Carbon Materials for Enhanced Oxygen Reduction Reaction Activity. *ACS Appl. Nano Mater.* **2018,** *1*, 1801-1810.

(25) Zhao, Y.; Wan, J.; Yao, H.; Zhang, L.; Lin, K.; Wang, L.; Yang, N.; Liu, D.; Song, L.; Zhu, J.; Gu, L.; Liu, L.; Zhao, H.; Li, Y.; Wang, D. Few-layer graphdiyne doped with sp-

hybridized nitrogen atoms at acetylenic sites for oxygen reduction electrocatalysis. *Nature Chemistry* **2018,** *10*, 924-931.

(26) Wang, Q.; Ji, Y.; Lei, Y.; Wang, Y.; Wang, Y.; Li, Y.; Wang, S. Pyridinic-N-dominated doped defective graphene as a superior oxygen electrocatalyst for ultrahigh-energy-density Zn-air batteries. *ACS. Energy. Lett.* **2018,** *3*, 1183-1191.

(27) Li, Z.; Zhuang, Z.; Lv, F.; Zhu, H.; Zhou, L.; Luo, M.; Zhu, J.; Lang, Z.; Feng, S.; Chen, W.; Mai, L.; Guo, S. The Marriage of the FeN4 Moiety and MXene Boosts Oxygen Reduction Catalysis: Fe 3d Electron Delocalization Matters. *Adv. Mater.* **2018,** *30*.

(28) Li, B.; Sasikala, S. P.; Kim, D. H.; Bak, J.; Kim, I.-D.; Cho, E.; Kim, S. O. Fe-N4 complex embedded free-standing carbon fabric catalysts for higher performance ORR both in alkaline & acidic media. *Nano Energy* **2019,** *56*, 524-530.

(29) Jiang, H.; Gu, J.; Zheng, X.; Liu, M.; Qiu, X.; Wang, L.; Li, W.; Chen, Z.; Ji, X.; Li, J. Defect-rich and ultrathin N doped carbon nanosheets as advanced trifunctional metal-free electrocatalysts for the ORR, OER and HER. *Energy Environ. Sci.* **2019,** *12*, 322-333.

(30) Han, H.; Noh, Y.; Kim, Y.; Jung, W. S.; Park, S.; Kim, W. B. An N-doped porous carbon network with a multidirectional structure as a highly efficient metal-free catalyst for the oxygen reduction reaction. *Nanoscale* **2019,** *11*, 2423-2433.

(31) Yang, L.; Xu, G.; Ban, J.; Zhang, L.; Xu, G.; Lv, Y.; Jia, D. Metal-organic framework-derived metal-free highly graphitized nitrogen-doped porous carbon with a hierarchical porous structure as an efficient and stable electrocatalyst for oxygen reduction reaction. *J. Colloid Interf. Sci.* **2019,** *535*, 415-424.

(32) Lv, Y.; Yang, L.; Cao, D. Sulfur, Nitrogen and Fluorine Triple-Doped Metal-Free Carbon

Electrocatalysts for the Oxygen Reduction Reaction. *Chemelectrochem* **2019,** *6*, 741-747.

(33) Yu, Y.; Zhang, Z.; Dai, L.; Wang, F. Copolymer-induced intermolecular charge transfer: Enhancing activity of metal-free catalysts for oxygen reduction. *Chem-Euro. J.* **2019,** *25*, 5652-5657.

(34) Gan, R.; Song, Y.; Ma, C.; Shi, J. In situ growth of N-doped carbon nanotubes in Fe-Nx/Fe_2O_3/Fe_3O_4-encapsulated carbon sheets for efficient bifunctional oxygen catalysis. *Appl. Catal. B-Environ.* **2023,** *327*, 122443-122452.

(35) Huang, Y.; Liu, K.; Kan, S.; Liu, P.; Hao, R.; Liu, W.; Wu, Y.; Liu, H.; Liu, M.; Liu, K. Highly dispersed Fe-Nx active sites on graphitic-N dominated porous carbon for synergetic catalysis of oxygen reduction reaction. *Carbon* **2021,** *171*, 1-9.

(36) Wang, X.; Gong, X.; Hu, L.; Fan, J.; Chen, R.; Jia, Y.; Cheng, Y.; Jiang, B.; Geng, H. Constructing Pt and Pt/MoC Co-anchored on nitrogen-doped carbon toward excellent methanol-resilient oxygen reduction performance for Zinc-Air batteries. *ChemNanoMat* **2023,** *9*, e202200365.

(37) Tang, C.; Wang, B.; Wang, H. F.; Zhang, Q. Defect engineering toward atomic Co-Nx-C in hierarchical graphene for rechargeable flexible solid Zn-air batteries. *Adv. Mater.* **2017,** *29*, 1703185-1703194.

(38) Yang, S.; Yu, Y.; Dou, M.; Zhang, Z.; Dai, L.; Wang, F. Two-dimensional conjugated aromatic networks as high-site-density and single-atom electrocatalysts for the oxygen reduction reaction. *Angew. Chem. Int. Ed.* **2019,** *58*, 14724-14730.